

Excitonic artificial atoms: Engineering optical properties of quantum dots

Pawel Hawrylak

*Technische Physik, Universitat Wurzburg, Am Hubland, D-97074 Wurzburg, Germany
and Institute for Microstructural Sciences, National Research Council of Canada, Ottawa, Canada K1A 0R6*

(Received 2 February 1999)

We investigate factors which control the optical properties of quantum dots filled with N excitons. Detailed calculation of the electronic structure of these excitonic artificial atoms is carried out for up to six excitons in a semianalytical fashion. The principle underlying the electronic structure of excitonic artificial atoms, the ‘‘hidden symmetry,’’ is discussed. The role of ‘‘hidden symmetry’’ in the emission spectrum as a fingerprint of the number of excitons in a quantum dot is analyzed in detail. [S0163-1829(99)14327-3]

I. INTRODUCTION

The many applications of artificially structured materials result from the controlled modification of their density of states. This modification has been consciously carried out at the one particle level by reducing the dimension of structures from three to zero. For electronic and optoelectronic applications, these nanostructures have to be filled with carriers. Reduced dimension implies an increase in interaction strength, and the density of states of a many-particle system need not resemble the one-particle density of states. Hence it is necessary to engineer not only one-particle levels but to carry this concept a step further, and engineer many-particle systems. The tools are now the number and structure of bound single-particle levels, the form of Coulomb interaction among carriers, and many-particle configurations which depend strongly on the number of carriers.

In the case of electronic devices such as quantum-dot (QD) single-electron transistors,¹ the finite electrostatic energy of adding an electron charge to the dot leads to a clear fingerprint of electron addition spectra in the form of Coulomb blockade.²⁻⁴ Optical devices, such as QD single-exciton lasers (QSXL),^{5,6} involve addition/subtraction of excitons. In contrast to electrons, excitons are charge neutral and their ‘‘removal/addition’’ spectra are less obvious. Bayer *et al.*⁷ carried out a detailed spectroscopy of a single etched quantum dot as a function of the excitation power (number of excitons) and the shape and size of a quantum dot, a clear first experimental attempt at engineering optical properties of zero-dimensional (0D) systems. Unfortunately, the estimated quantization of single-particle energies, smaller than the 2D excitonic binding energy, precludes a reliable many-exciton calculation. Nevertheless, experimental emission spectra did reveal sensitivity to the number of excitons in the dot, with qualitative features which could be interpreted in terms of a strongly quantized system. The authors of Refs. 8, 9, and 10 have successfully manipulated shapes and sizes of self-assembled quantum dots (SAD) showing promising optical properties.

For these reasons a detailed fingerprint of the exciton removal (emission) spectrum as a function of the number N of excitons is needed. Calculations of many-exciton states have been carried out in Refs. 11–13 using exact diagonalization techniques. In Ref. 11 a model asymmetric quantum box was

investigated. The box allowed two nondegenerate orbital levels per electron and hole, and could accommodate up to four excitons. In Refs. 12 and 13, quantum dots with degenerate electronic shells were investigated for up to twenty excitons. The key physics was found to be associated with excitons occupying degenerate electronic orbitals. The results of Refs. 12 and 13 revealed an underlying principle of single-exciton devices, the ‘‘hidden symmetry.’’ Hidden symmetries involve both single-particle levels and interparticle interactions. Engineering both leads to a complete control of optical spectra of excitonic artificial atoms as a function of the number of excitons N . In order to achieve such control a good, and if possible analytical, understanding of what determines these spectra is needed. We carry out such a program here by calculating the few exciton states in a parabolic quantum dot. These semianalytical calculations clarify the ‘‘hidden symmetry’’ principle underlying the emission/addition spectra of QSXL in terms of more familiar direct, exchange, and correlation effects.

At present most single-dot recombination experiments^{7,14-16} have been carried on dots with up to four excitons. We therefore limit our work here to spectra of not more than six excitons in quantum dots with large confinement energy and few confined states. The model is sufficiently general to apply to all dots with large quantization of kinetic energy and cylindrical symmetry.

II. SINGLE-PARTICLE STATES

As a representative example we start with the single-particle states of self-assembled indium-based quantum dots. These states are determined by many factors, such as shape, indium-concentration profile, conduction- and valence-band offsets, strain, deviation from equilibrium, and degree of faceting, none of them known independently. To complicate matters, InAs is a narrow gap material with coupling of valence- and conduction-band states. Hence, while calculations of single-particle levels are very involved,^{17,18} they must in the end lead to a small number of bound states.

High excitation photoluminescence,¹³ capacitance, far-infrared absorption measurements,^{19,20} and numerical calculations²¹ indicate that in lens-shaped quasi-two-dimensional SAD's the bound states of both electrons and valence-band holes can be understood assuming an effective

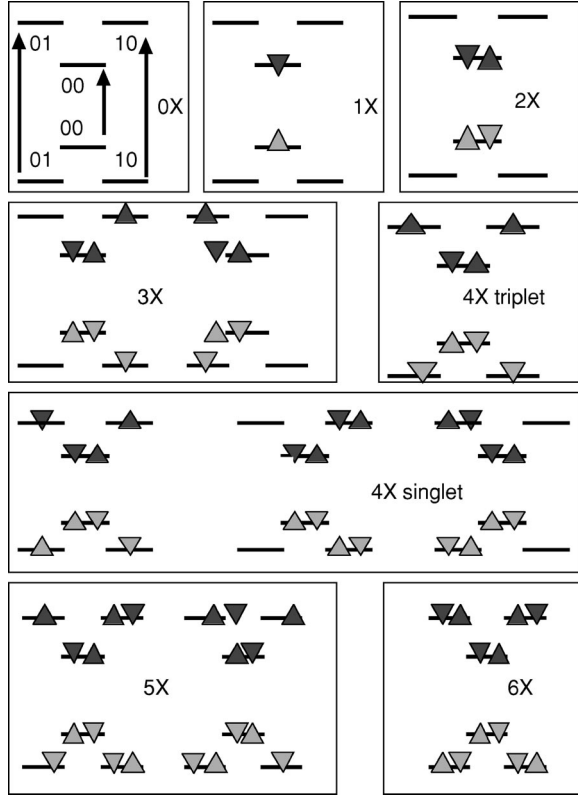


FIG. 1. Lowest-kinetic-energy configurations of from zero to six excitons.

parabolic potential. The single particle levels then correspond to the levels of two harmonic oscillators.^{1,22} The electronic energies $E_{mn}^e = \Omega_+^e(n + \frac{1}{2}) + \Omega_-^e(m + \frac{1}{2})$, eigenstates $|mn\rangle$ and angular momenta $L_{mn}^e = m - n$ are those of two harmonic oscillators tunable with the magnetic field B applied normal to the plane of the dot. The frequencies $\Omega_{+/-} = \frac{1}{2}(\sqrt{\omega_c^2 + 4\omega_0^2} \pm \omega_c)$, where $\omega_c = eB/m^*c$ is the cyclotron energy, m^* is the effective mass, and e is the charge of an electron. The magnetic length l_0 is given by $l_0 = 1/\sqrt{m^*\omega_c}$, and the effective length $l_{\text{eff}} = 1/[1 + (4\omega_0^2/\omega_c^2)]^{1/4}$. The splitting of different spin σ energy levels (Zeeman energy) is very small compared to other energies.

The valence hole states are Luttinger spinors. The spinor nature leads to interesting and nontrivial effects involving hole-hole interactions.²³ However, in strained structures the splitting of heavy and light holes is expected to remove some of these complications and justify the use of the one-band effective-mass approximation. Hence a valence-band hole is treated in the effective-mass approximation as a positively charged particle with angular momentum $L_{mn}^h = n - m$, opposite to the electron, and energies $E_{mn}^h = \Omega_+^h(n + \frac{1}{2}) + \Omega_-^h(m + \frac{1}{2})$ (ignoring the semiconductor gap E_G).

An example of the single particle spectrum of a two-shell quantum dot is shown in Fig. 1. The two lowest shells are the same for all quantum dots with cylindrical symmetry.

III. HAMILTONIAN AND COULOMB MATRIX ELEMENTS

With a composite index $j = [m, n, \sigma]$, the Hamiltonian of the interacting electron-hole system may be written in a compact form as

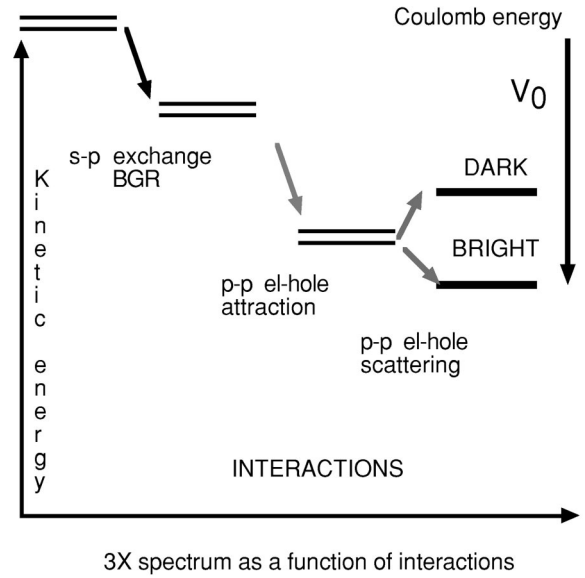


FIG. 2. Contributions to energy levels and oscillator strength of the three exciton complex.

$$\begin{aligned}
 H = & \sum_i E_i^e c_i^+ c_i + \sum_i E_i^h h_i^+ h_i - \sum_{ijkl} \langle ij | V_{\text{eh}} | kl \rangle c_i^+ h_j^+ h_k c_l \\
 & + \frac{1}{2} \sum_{ijkl} \langle ij | V_{\text{ee}} | kl \rangle c_i^+ c_j^+ c_k c_l \\
 & + \frac{1}{2} \sum_{ijkl} \langle ij | V_{\text{hh}} | kl \rangle h_i^+ h_j^+ h_k h_l.
 \end{aligned} \quad (1)$$

The operators c_i^+ (c_i) and h_i^+ (h_i) create (annihilate) the electron or valence-band hole in the state $|i\rangle$ with the single-particle energy E_i . The two-body Coulomb matrix elements are $\langle ij | V | kl \rangle$ for electron-electron (ee), hole-hole (hh), and electron-hole (eh) scattering, respectively.^{24,25} Coulomb matrix elements are measured here in units of $V_0 = \text{Ry} \sqrt{\pi a_B} / l_{\text{eff}}$, where Ry is the effective Rydberg and a_B is the effective Bohr radius. At zero magnetic field the effective length $l_{\text{eff}} = 1/\sqrt{2\omega_0 m^*}$ and $V_0 = \text{Ry} \sqrt{\pi a_B} \sqrt{2\omega_0 m^*}$. Hence a typically smaller confining potential for holes can be compensated for by their heavy mass, and the strength of electron-electron and hole-hole interactions can be equal. The scaling of interaction with single particle spacing implies that for spacing $\omega_0/\text{Ry} > \pi$ kinetic energy dominates, and effects of interactions involving intershell transitions can be treated perturbatively. For states forming degenerate shells, Coulomb interactions completely determine the spectrum.

The Coulomb matrix elements depend on the form of single-particle states and the form of interaction. The interaction can be controlled independently of single-particle states. For example, an application of perpendicular electric field may either separate or bring together electrons and holes, and weaken or strengthen the electron-hole interaction in comparison with the electron-electron interactions. Therefore one can achieve a situation where all direct ee, hh, and eh matrix elements $\langle i; j | V | j; i \rangle$ are equal. Moreover, the electron-hole scattering matrix elements $\langle i; i | V_{\text{eh}} | j; j \rangle$ can be made equal in magnitude to ee and hh exchange matrix ele-

ments $\langle i; j | V_{ee} | i; j \rangle$. This ‘‘symmetrical’’ case will be our starting point, with possible departures treated perturbatively for particular structures.

We restrict our attention to the two lowest shells s and p , and symmetric interactions. Below we list relevant Coulomb matrix elements in units of their respective V_0 : $\langle 00; 00 | V | 00, 00 \rangle = 1.0000$, $\langle 10; 00 | V | 00, 10 \rangle = 0.7500$, and $\langle 10; 10 | V | 10, 10 \rangle = 0.6875$. To elucidate the physics, we shall refer to the matrix elements by also specifying which type of carrier, which shell, and whether direct or exchange scattering is involved. For example, $V_{ee}^{pp,x}$ denotes electron-electron exchange scattering involving two electrons on a p shell. The p -shell electron hole scattering matrix elements V_{eh}^{pp} are equal to equivalent ee exchange matrix elements $V_{ee}^{pp,x}$, $\langle 10; 10 | V_{eh} | 01, 01 \rangle = 0.1875 = \langle 10; 01 | V_{ee} | 10, 01 \rangle$. The p - to s -shell electron-hole scattering matrix elements V_{eh}^{ps} are equal to equivalent ee exchange matrix elements $V_{ee}^{ps,x}$, $\langle 10; 10 | V_{eh} | 00, 00 \rangle = 0.2500 = \langle 10; 00 | V_{ee} | 10, 00 \rangle$. This list of Coulomb matrix elements illustrates the relative importance of different processes.

We must now construct states of the electron-hole system. We can classify states by the total angular momentum $L = L_e + L_h$ and by the z component of the total spin $S_z = S_z^e + S_z^h$. Moreover, since electron-hole scattering does not change the total spin of the electron or hole system, we can classify our states by the total spin S of each component. We label all possible electronic (hole) states in a Hilbert space with a given total spin, z th component, and angular momentum. The wave function of the system of electrons and holes is spanned by a set of $l \times k$ basis states belonging to Hilbert spaces labeled by L, S_z, S_e, S_h :

$$|L_e, S_z^e, S_e, k\rangle |L_h, S_z^h, S_h, l\rangle. \quad (2)$$

The interband optical processes in a quantum dot are described by the set of interband polarization operators P_σ^+ (P_σ^-) which create (annihilate) electron-hole pairs with definite spin configuration $P_\sigma^+ = \sum_i c_i^+ h_{i,-\sigma}^+$ ($P_\sigma^- = \sum_i h_{i,-\sigma} c_{i\sigma}$) by annihilating (creating) photons with definite circular polarization.¹² The remaining electron-hole pair spin configurations (σ, σ) correspond to dark excitons. The third component $P_z = \frac{1}{2}(N_\sigma^e + N_\sigma^h - N_{\text{tot}})$ measures population inversion, i.e., a number of excitons $N_\sigma = N_\sigma^e = N_\sigma^h$ with definite spin σ in N_{tot} of the single-particle levels. P satisfies commutation relations of a 3D angular momentum $[P^+, P^-] = 2P_z$, $[P_z, P^\pm] = \pm P^\pm$. The total polarization $P^2 = \frac{1}{2}(P^+ P^- + P^- P^+) + P_z^2$ commutes with P^+ .

The dynamics of the polarization operator (neglecting the spin degrees of freedom) is given by the commutator of P^+ with the Hamiltonian:¹²

$$\begin{aligned} [H, P^+] = & \sum_i (E_i^e + E_i^h) c_i^+ h_i^+ - \sum_{ijk} \langle ij | V_{eh} | kk \rangle c_i^+ h_j^+ \\ & + \frac{1}{2} \sum_{ijkl} (\langle ij | V_{ee} | kl \rangle - \langle ik | V_{eh} | jl \rangle) (c_i^+ h_l^+ c_j^+ c_k \\ & - c_i^+ h_k^+ c_j^+ c_l) + \frac{1}{2} \sum_{ijkl} (\langle ij | V_{hh} | kl \rangle - \langle ik | V_{eh} | jl \rangle) \end{aligned}$$

$$\times (c_l^+ h_i^+ h_j^+ h_k - c_k^+ h_i^+ h_j^+ h_l). \quad (3)$$

The dynamics of the interband polarization requires the knowledge of both two- and four-particle operators, the dynamics of which has to be sought and truncated at some level of approximation. However, as is clearly evident from Eq. (3) and demonstrated in Ref. 12, the degeneracy of single-particle levels ($E_i^e + E_i^h$) and the symmetry of ee, hh, and eh interactions cause both a remarkable cancellation of the four-particle contribution and lead to a very simple dynamics of the interband polarization operator operating on a degenerate shell, $[H, P^+] = E_X P^+$, where E_X is the exciton energy for a given shell.

The energy of states on a given shell generated from the vacuum by a multiple application of P^+ , $|N\rangle = (P^+)^N |v\rangle$, depends linearly on N , i.e., on the number of excitons. Hence the energy of addition/subtraction of excitons from these states does not depend on the number of excitons. This is the essence of ‘‘hidden symmetry.’’ Therefore, emission from degenerate states takes place at the same energy, and we cannot determine the number of excitons in a given shell. For this we need excited states. We shall now discuss how this degeneracy takes place, what is the role of spin, and what are the excited states by explicit construction of many-exciton states and diagonalization of the Hamiltonian.

IV. EXCITONIC GROUND STATES

We consider the simplest possible N -excitonic states (NX), i.e., states built only out of the lowest kinetic energy states of N electron-hole pairs. The lowest-kinetic-energy states are obtained by populating the lowest-kinetic-energy single-particle levels of each type of carrier according to the Pauli exclusion principle. Because the kinetic energy $t = \Omega^e + \Omega^h$ is proportional to ω_0 , and the Coulomb energy V_0 is proportional to $\sqrt{\omega_0}$, the small parameter in our calculations is the ratio of Coulomb to kinetic energy. Hence the lowest-kinetic-energy states should approach exact states in the limit of $V_0/t \rightarrow \infty$, i.e., large confinement.

A. One- and two-exciton complexes

One exciton corresponds to an electron and a hole occupying their lowest-kinetic-energy state $|00, \downarrow\rangle |00, \uparrow\rangle$, as shown in Fig. 1. We have adopted a convention in which optically allowed electron and hole states have zero total S_z . The spin has been incorporated in this figure by using triangles, e.g., triangles pointing up correspond to spin-up particles. Pairs of particles with total spin, i.e., $|\uparrow\rangle |\uparrow\rangle$ and $|\downarrow\rangle |\downarrow\rangle$ form spin-dark excitons.

The exciton energy is simply given by the electron plus the hole kinetic energy and their mutual attraction:

$$E_s^0 = \Omega^e + \Omega^h - \langle 00; 00 | V_{eh} | 00; 00 \rangle. \quad (4)$$

The exciton state is doubly degenerate due to spin.

For the two-exciton complex there is only one lowest-kinetic-energy configuration, shown in Fig. 1, the singlet-singlet configuration $|XX\rangle = c_{00\uparrow}^+ c_{00\downarrow}^+ h_{10\uparrow}^+ h_{00\downarrow}^+ |v\rangle$, where $|v\rangle$

is the vacuum. This configuration corresponds to a product of the electron and hole singlet states.

The biexciton energy is twice the single exciton energy plus a Hartree term due to possible differences in electron and hole charge distribution:

$$E_{2X}^0 = 2E_s^0 + 2[\langle 00;00|V_{ee}|00;00\rangle - \langle 00;00|V_{eh}|00;00\rangle]. \quad (5)$$

Hence in the ideal limit of very strong confinement and symmetric interactions the biexciton energy is exactly twice the exciton energy, i.e., there is no binding energy. This is simply because binding, or lowering, of energy comes from the scattering to available states, and here there are none. Hence we expect the biexciton binding energy to increase from the 2D value with increasing confinement, but eventually decrease to zero when the quantization of single-particle energy by far exceeds the exciton binding energy.

In the strong confinement limit, deviations may come from the asymmetry of interactions, and may be interpreted as either exciton binding or repulsion, depending on whether the electron-hole attraction is weaker than or equal to the electron-electron repulsion. The second correction will come from scattering to higher shells. Since there is only one singlet for electrons and one singlet for holes, the ground state is not degenerate, and there are no dark biexciton states due to spin.

B. Three excitons

There are two lowest-energy three-exciton configurations $|a\rangle$ and $|b\rangle$, shown in Fig. 1. The extra electron hole pair can be in either of the two degenerate p states: $|a\rangle = c_{10\downarrow}^+ h_{10\uparrow}^+ |XX\rangle$ and $|b\rangle = c_{01\downarrow}^+ h_{01\uparrow}^+ |XX\rangle$. The energy E_p , measured from the $2X$ state $2E_s^0$, is a sum of a number of terms:

$$E_p = (2t - [V_{ee}^{sp,x} + V_{hh}^{sp,x}] - V_{eh}^{pp,d}). \quad (6)$$

The first term is the kinetic energy, the second term is the band-gap renormalization due to exchange of the p -shell electron (hole) with like-spin electron (hole) in the filled s -shell. The third term is the direct attraction between the electron and the hole in the same orbital of the p shell.

The electron-hole interaction V_{eh}^{pp} allows the electron-hole pair to scatter from the $(1,0)(1,0)$ state to the $(0,1)(0,1)$ state, and mixes the two configurations. The two solutions can be obtained analytically. We insert values of respective matrix elements to illustrate the strength of different contributions to the ground- and excited-state energies:

$$E_{3X}^{\pm} = 2E_s^0 + (2t - 0.5V_0 - 0.6875V_0) \pm (-0.1875V_0). \quad (7)$$

The ground-state energy is $E_{3X} = 2E_s^0 + (2t - 1.375V_0)$. The interaction energy contribution to the energy of the extra

p electron ($-1.375V_0$) is larger than the interaction energy of the one exciton state ($-1.00V_0$) due to exchange with the filled s shell.

The two eigenstates are $|\pm\rangle = (|a\rangle \pm |b\rangle)/\sqrt{2}$. Since the ground state $|+\rangle$ is proportional to the interband polarization operator $P^+ = \sum_{i,\sigma} c_{i\sigma}^+ h_{i-\sigma}^+$, it is optically active. The second state $|-\rangle$ is dark due to parity. It can be made active by a perturbation removing the degeneracy of the two p states, e.g., loss of circular symmetry, perpendicular magnetic field, or in-plane electric field. However, the spectrum should still be dominated by the symmetric state. So starting from the two optically active configurations $|a\rangle$ and $|b\rangle$, by allowing for electron-hole scattering we arrived at only one active configuration. A summary of different mechanisms leading to energy levels and oscillator strengths of the bright and dark three exciton complexes is shown in Fig. 2. The spin structure, degeneracies, and spin-dark excitons are identical to a single exciton case.

C. Four excitons

The four-exciton complex can be in different total spin arrangements of the partially filled p shell electrons and holes, the triplet-triplet, the singlet-singlet configuration, and the singlet-triplet configurations. There are nine possible degenerate triplet-triplet states, only three of them optically active.

Let us first discuss the triplet-triplet configuration, $|t\rangle = (c_{10\downarrow}^+ h_{10\uparrow}^+)(c_{01\downarrow}^+ h_{01\uparrow}^+) |XX\rangle$ as shown in Fig. 1. We have written this state explicitly as a product of two electron-hole pairs. The energy of each pair is the same as the energy E_p of a single pair in the $3X$ complex. However, two electrons and two holes have parallel spins and lower their respective energy by exchange. The ground-state energy, measured from the energy $2E_s^0$ of the filled s shell, is

$$E_{4Xt} = (2[2t - (V_{ee}^{sp,x} + V_{hh}^{sp,x}) - V_{eh}^{pp,d}] - (V_{ee}^{pp,x} + V_{hh}^{pp,x})). \quad (8)$$

Because exchange interaction and electron-hole scattering interactions are equal and attractive, $V_{ee}^{pp,x} = V_{eh}^{pp}$, the energy of the two additional excitons in a p shell of the four exciton complex is exactly twice the energy of a single exciton in a three exciton complex, $E_{4Xt} = 2E_{3X}$. This is so because the lowering of energy due to mixing of electron-hole configurations of the three exciton complex is exactly equal to the exchange energy in a single four-exciton configuration. Seemingly very different mechanisms lead to a very simple result, i.e., that the energy to add an electron-hole pair does not depend on the number of pairs already present. While it is perhaps not too difficult to understand why this happens for a spin-polarized system with only one configuration, we will show that the same degeneracy happens in a ground state of the singlet-singlet configuration.

When both electrons and holes are in singlet configurations, the total number of possible configurations increases. While there was only one triplet-triplet configuration, there are three possible singlet-singlet configurations, as shown in Fig. 1:

$$|a\rangle = (c_{10\uparrow}^+ c_{10\downarrow}^+) (h_{10\downarrow}^+ h_{10\uparrow}^+) |XX\rangle,$$

$$|b\rangle = \frac{1}{\sqrt{2}} (c_{10\uparrow}^+ c_{01\downarrow}^+ + c_{01\uparrow}^+ c_{10\downarrow}^+) \frac{1}{\sqrt{2}} (h_{10\downarrow}^+ h_{01\uparrow}^+ + h_{01\downarrow}^+ h_{10\uparrow}^+) |XX\rangle, \quad (9)$$

$$|c\rangle = (c_{01\uparrow}^+ c_{01\downarrow}^+) (h_{01\downarrow}^+ h_{01\uparrow}^+) |XX\rangle.$$

By comparing Fig. 1 and Eq. (9), we see that the singlet-singlet configuration is actually a mixture of four configurations, two involving electrons and holes with spin different from zero, and hence dark.

It is also clear that electron-hole scattering can move an electron-hole pair from configuration $|b\rangle$ to either configuration $|a\rangle$ or $|c\rangle$. This matrix element $\langle a|H|b\rangle$ equals the electron-hole scattering matrix element V_{eh}^{pp} times the product of the normalization factors of states $|a\rangle$ and $|b\rangle$, equal to 2. Hence the effective scattering from a to b is twice the single pair scattering. The energy of configurations $|a\rangle$ and $|c\rangle$ is just the sum of pair energy, i.e., $2E_p$. The energy of configuration $|b\rangle$ is increased by repulsive exchange energy $2E_p + (V_{ee}^{pp,x} + V_{hh}^{pp,x})$ of singlet p -shell electrons and holes.

We can now write the Hamiltonian for the singlet-singlet states:

$$\begin{pmatrix} 2E_p & -2V_{eh}^{pp} & 0 \\ -2V_{eh}^{pp} & 2E_p + 2V_{ee}^{pp,x} & -2V_{eh}^{pp} \\ 0 & -2V_{eh}^{pp} & 2E_p \end{pmatrix}.$$

We again utilize the fact that exchange interaction, repulsive here, is equal in magnitude to the attractive electron-hole scattering to obtain the three eigenvalues expressed solely in terms of electron-hole matrix elements: $E_{4Xs}(1) = 2E_p - 2V_{eh}^{pp}$, $E_{4Xs}(2) = 2E_p$, and $E_{4Xs}(3) = 2E_p + 4V_{eh}^{pp}$. The respective eigenvectors are $|1\rangle = (1/\sqrt{3})(|a\rangle + |b\rangle$

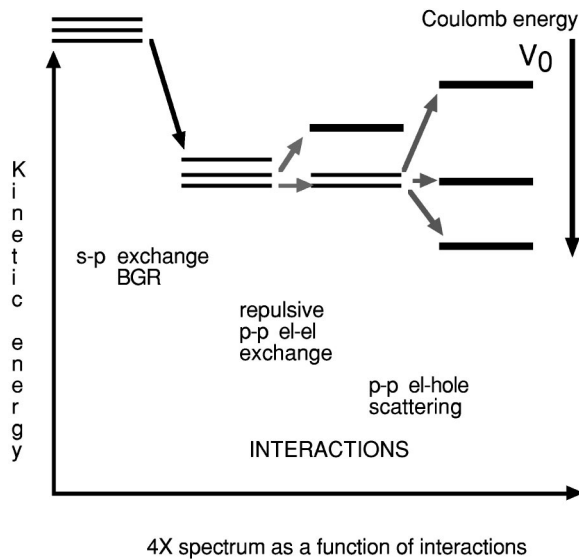


FIG. 3. Contributions to energy levels and oscillator strength of the singlet-singlet four exciton complex.

$+ |c\rangle$), $|2\rangle = (1/\sqrt{2})(-|a\rangle + |c\rangle)$, and $|3\rangle = (1/\sqrt{6})(|a\rangle - 2|b\rangle + |c\rangle)$. We see that $E_{4Xs}(1) = 2(E_{3X})$, i.e., the energy of the lowest singlet-singlet state is twice the energy of the single exciton in a p shell. The singlet-singlet and triplet-triplet configurations are degenerate.

We can conclude here that for spin-polarized configurations there are few states (one triplet-triplet in this example). Their energy is reduced by attractive exchange interaction among like particles. For spin-unpolarized configurations there are many more available configurations (three singlet-singlet configurations in this example). The energy of these individual configurations is increased by exchange, but correlations due to mixing of these states by electron-hole scattering more than compensate for the repulsive exchange energy and reduce the ground-state energy. To underscore different mechanisms leading to this result, a schematic evolution of the four exciton states as a function of interactions is shown in Fig. 3.

Let us now see which of the eigenvalues is optically active, i.e., from which an exciton can be removed. Let us define an operator removing a p -shell exciton: $P_p^- = h_{(0,1),\uparrow} c_{(0,1),\downarrow} + h_{(1,0),\downarrow} c_{(1,0),\uparrow}$. The symmetric lowest-energy $3X$ configuration, labeled by the spin of an electron σ , can be written as $|3X, +, \sigma\rangle = (1/\sqrt{2}) P_{p,\sigma}^+ |XX\rangle$.

Applying P_p^- to the three eigenstates we find $P_p^- (|a\rangle + |c\rangle) = P_p^+ |XX\rangle$ and $P_p^- |b\rangle = \frac{1}{2} P_p^+ |XX\rangle$. Hence we see that removing an exciton from the lowest eigenvalue $|1\rangle$ gives the two $3X$ symmetrical states $P_p^- |1\rangle = (\sqrt{3}/\sqrt{2}) \sum_{\sigma} |3X, +, \sigma\rangle$. The amplitude of the removal process, $\sqrt{3}/\sqrt{2}$, is a ratio of the normalization constant of the initial and the final state.

Removing an exciton from the second eigenvalues gives $P_p^- |2\rangle = P_p^- (|a\rangle - |c\rangle) = \sum_{\sigma} |3X, -, \sigma\rangle$, which is the sum of

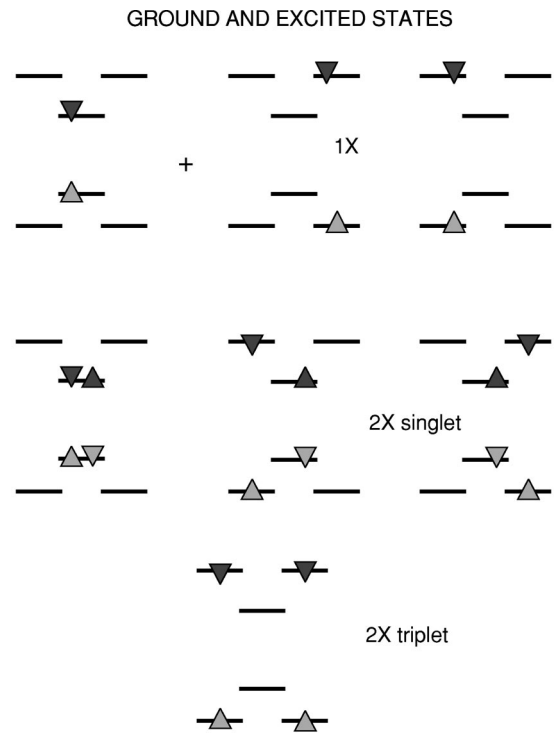


FIG. 4. Lowest-kinetic-energy excited configurations of one and two excitons.

the two dark antisymmetric excited $3X$ states. Hence an excited $4X$ state can recombine by emitting a photon to a dark excited $3X$ final state. The energy of this transition will turn out to be degenerate with the energy of the ground-state to ground-state transition. Removing an exciton from the highest eigenvalue gives $P^-|3\rangle = P^- (|a\rangle + |c\rangle) - P^-(2|b\rangle) = 0$. Hence this state cannot recombine via a radiative process.

Let us now discuss singlet-triplet combinations. Since triplet states have zero total angular momentum, only zero angular momentum singlet combination is possible, and we can form only one state:

$$|a\rangle = \frac{1}{\sqrt{2}}(c_{10\uparrow}^+ c_{01\downarrow}^+ + c_{01\uparrow}^+ c_{10\downarrow}^+)(h_{10\downarrow}^+ h_{01\uparrow}^+) |XX\rangle. \quad (10)$$

The energy of this state, $E_a = 2E_s^0 + 2E_p$, equals the energy of the first excited state of the singlet-singlet configuration. In this state the repulsive exchange in electronic singlet was canceled by the attractive exchange in a triplet hole configuration.

Removing an exciton from this state leaves a $3X$ state which is dark due to spin arrangement and due to parity (antisymmetric state). The energy of the final state is the energy of the $|3X-\rangle$ state. Because both the initial and final states have higher energy, the transition energy, i.e. the energy to remove an exciton from this state is identical to the energy required to remove an exciton from either singlet-singlet or triplet-triplet configuration.

V. FIVE AND SIX EXCITONS

The analysis of the states of five excitons is analogous to the analysis of the $3X$ state. There are two states, one dark, and one bright, with energy $E = 2E_s^0 + 3E_{3X}$. There is only one six exciton state and its energy is again a linear function of the number of excitons in a p shell, $E = 2E_s^0 + 4E_{3X}$.

VI. EXCITED STATES AND CORRECTIONS TO THE GROUND STATE

We now investigate excited states and their effect on the N -exciton ground state. The excited states can be classified by their kinetic energy. The lowest-kinetic-energy excited states involve promoting only one exciton at a time to a higher shell. Figure 4 shows the lowest excited states of $1X$ and $2X$ complexes. Let us first discuss the $1X$ state.

A. Exciton

The wave function can be written as a linear combination of three states: the lowest-kinetic-energy state $|0\rangle = c_{00\downarrow}^+ h_{00\uparrow}^+ |v\rangle$ and the two excited states $|a\rangle = c_{10\downarrow}^+ h_{10\uparrow}^+ |v\rangle$ and $|b\rangle = c_{01\downarrow}^+ h_{01\uparrow}^+ |v\rangle$. Following our analysis of the $3X$ case we first form a symmetric (+) and antisymmetric (-) combination of states $|a\rangle$ and $|b\rangle$. Only the symmetric combination $|+\rangle$, couples to the lowest-kinetic-energy exciton state. The final Hamiltonian is easily solved analytically, and for clarity here we write all numerical coefficients explicitly:

$$\begin{pmatrix} t - V_0 & -\sqrt{2}(0.25V_0) & 0 \\ -\sqrt{2}(0.25V_0) & 2t - 0.6875V_0 - 0.1875V_0 & 0 \\ 0 & 0 & 2t - 0.6875V_0 + 0.1875V_0 \end{pmatrix}.$$

We find that for $V_0/t = 0.5$ the change in the exciton ground state is only 6% of the kinetic energy t , while for $V_0/t = 1$ it is 10% of t .

B. Two excitons

The ground state of two excitons is a singlet but excited states also include a triplet configuration, as shown in Fig. 4. Corrections to the singlet ground state come only from singlet excited states. There are three states, shown schematically in Fig. 4:

$$|0\rangle = (c_{00\uparrow}^+ c_{00\downarrow}^+)(h_{00\downarrow}^+ h_{00\uparrow}^+) |v\rangle,$$

$$|a\rangle = \frac{1}{\sqrt{2}}(c_{10\uparrow}^+ c_{00\downarrow}^+ + c_{00\uparrow}^+ c_{10\downarrow}^+) \frac{1}{\sqrt{2}}(h_{10\downarrow}^+ h_{00\uparrow}^+ + h_{00\downarrow}^+ h_{10\uparrow}^+) |v\rangle, \quad (11)$$

$$|b\rangle = \frac{1}{\sqrt{2}}(c_{01\uparrow}^+ c_{00\downarrow}^+ + c_{00\uparrow}^+ c_{01\downarrow}^+) \frac{1}{\sqrt{2}}(h_{01\downarrow}^+ h_{00\uparrow}^+ + h_{00\downarrow}^+ h_{01\uparrow}^+) |v\rangle.$$

The energy of configuration (0) is just $2E_s^0$, the energy of configurations (a) and (b) is a sum of the electron-hole pair in the s orbital E_s^0 and in the p orbital $E_a = E_s^0 + E_p^0 + (V_{ee}^{sp,x} + V_{hh}^{sp,x})$, where E_p^0 is the energy of electron-hole pair in the p orbital but without exchange interaction with a filled s shell. The last term is the repulsive exchange term coming from the singlet character of the orbital wave function. These configurations are mixed by electron-hole scattering, with coefficients modified by the form of each wave function. We again form first a symmetric (+) and antisymmetric (-) linear combinations of configurations (a) and (b). In this basis, the Hamiltonian

$$\begin{pmatrix} E_s^0 + E_s^0 & -2\sqrt{2}V_{eh}^{sp} & 0 \\ -2\sqrt{2}V_{eh}^{sp} & E_s^0 + E_p^0 + (V_{ee}^{sp,x} + V_{hh}^{sp,x}) - V_{eh}^{pp} & 0 \\ 0 & 0 & E_s^0 + E_p^0 + (V_{ee}^{sp,x} + V_{hh}^{sp,x}) + V_{eh}^{pp} \end{pmatrix}$$

can be diagonalized exactly.

For completeness we insert all numerical values of coulomb matrix elements to obtain the final form of the $2X$ Hamiltonian:

$$\begin{pmatrix} 2(t - V_0) & -2\sqrt{2}(0.25V_0) & 0 \\ -2\sqrt{2}(0.25V_0) & (t - V_0) + (2t - 0.1875V_0) - 0.1875V_0 & 0 \\ 0 & 0 & (t - V_0) + (2t - 0.1875V_0) + 0.1875V_0 \end{pmatrix}.$$

We find that the scattering to the p shell lowers the energy of the $2X$ complex by $0.089t$ for $V_0/t=0.5$, and by $0.264t$ for $V_0/t=1.0$. At the same time the exciton also lowers its energy. The $2X$ complex always has lower energy than the two noninteracting excitons, but the gain is very small. At $V_0/t=1.0$ we find the exciton energy shifted from its noninteracting value by $1.1t$, and the $2X$ energy by $2.26t$. These shifts are very large, i.e., of the order of 50–100 meV. At the same time the ‘binding energy’ $E_{XX} - 2E_X = 0.06t$ is very small, i.e., 3 meV for $t = 50$ meV.

We now turn to the triplet-triplet $2X$ state. The triplet biexciton involves spin-polarized electron (hole) pairs, one in the s shell and the second one in the p shell. The p electron can be in two different states, hence we have two triplet states

$$\begin{aligned} |a\rangle &= \frac{1}{\sqrt{2}}(c_{10\uparrow}^+ c_{00\downarrow}^+ - c_{00\uparrow}^+ c_{10\downarrow}^+) \frac{1}{\sqrt{2}}(h_{10\downarrow}^+ h_{00\uparrow}^+ - h_{00\downarrow}^+ h_{10\uparrow}^+), \\ |b\rangle &= \frac{1}{\sqrt{2}}(c_{01\uparrow}^+ c_{00\downarrow}^+ - c_{00\uparrow}^+ c_{01\downarrow}^+) \frac{1}{\sqrt{2}}(h_{01\downarrow}^+ h_{00\uparrow}^+ - h_{00\downarrow}^+ h_{01\uparrow}^+). \end{aligned} \quad (12)$$

The energy of configurations $|a\rangle$ and $|b\rangle$ is a sum of the energy of the electron-hole pair in the s orbital E_s^0 and in the p orbital, $E_a = E_s^0 + E_p^0 - (V_{ee}^{sp,x} + V_{hh}^{sp,x})$. The last term is the attractive exchange term coming from the triplet orbital wave function of electrons and holes. These configurations are mixed by electron-hole scattering. We again form first a symmetric (+) and antisymmetric (-) linear combinations of orbitals (a) and (b). In this basis the Hamiltonian is diagonal, and the two energies are $E_{2Xt}^\pm = E_s^0 + E_p^0 - (V_{ee}^{sp,x} + V_{hh}^{sp,x}) \pm (-V_{eh}^{pp})$. The lowest energy corresponds to a symmetric configuration, with numerical values of each contribution as $E_{2Xt}^+ = (t - V_0) + (2t - 0.6875V_0) - 0.5V_0 - 0.1875V_0$ and a final result $E_{2Xt}^+ = 3t - 2.375V_0$.

C. Three excitons

Three excitons turn out to be the most complicated case. The two lowest-energy configurations, shown in Fig. 5, are $|a\rangle = c_{10\downarrow}^+ h_{10\uparrow}^+ |XX\rangle$ and $|b\rangle = c_{01\downarrow}^+ h_{01\uparrow}^+ |XX\rangle$. They consist of

singlets in s orbitals and one electron in the p orbital, i.e., the total angular momentum of electrons is ± 1 . This momentum can be compensated for by only one identical hole configuration. The same argument applies to configurations Figs. 5(c) and 5(d)], where the total angular momentum of electrons is ± 2 . However, electron configurations [Figs. 5(e), 5(f), and 5(g)] all belong to the zero total electron angular momentum subspace. These configurations correspond to the motion of the spin-up electron, circulating on a plaquette of three inequivalent sites filled with spin-down electrons.²² Each of these electronic configurations can be paired with any of the identical hole configurations [Figs. 5(e), 5(f), and 5(g)] leading to a band of nine degenerate states. The nine states, plus the four singlet states, result in a total of 13 states. This problem unfortunately has to be solved numerically but we can obtain insight into the interesting band of spin-related 11 excited states by proceeding with analytical calculations.

We proceed by diagonalizing the electron part of the Hilbert space. Only three states [Figs. 5(e)–5(g)] are coupled by ee interaction, and the three eigenstates are²²

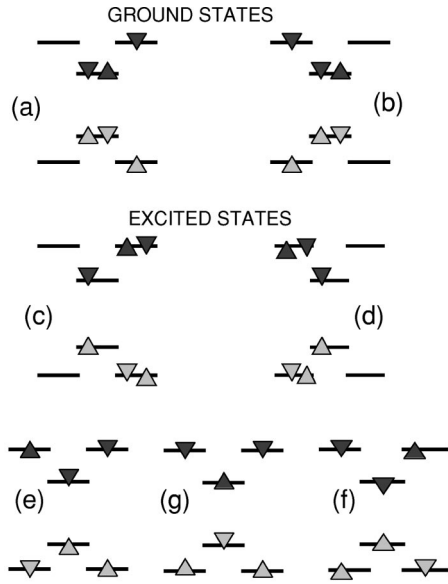


FIG. 5. Lowest-kinetic-energy excited configurations of three excitons.

$$\begin{aligned}
 |1\rangle &= \frac{1}{\sqrt{6}}(|e\rangle - 2|f\rangle + |g\rangle), \\
 |2\rangle &= \frac{1}{\sqrt{2}}(-|e\rangle + |g\rangle), \\
 |3\rangle &= \frac{1}{\sqrt{3}}(|e\rangle + |f\rangle + |g\rangle).
 \end{aligned} \tag{13}$$

These states have to be combined with identical hole states into nine products $|1\rangle|1'\rangle, |1\rangle|2'\rangle, \dots$. The six different energies are given by

$$E_{1,1} = E_s^0 + 2E_p^0 + 2V_{ee}^{pp,x} - 4V_{ee}^{sp,x},$$

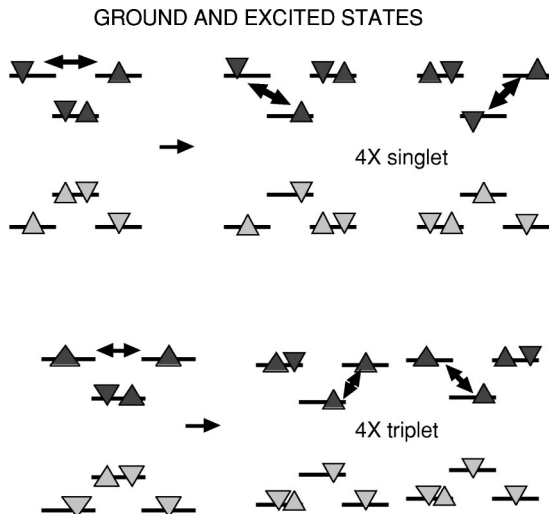


FIG. 6. Lowest-kinetic-energy excited configurations of four excitons.

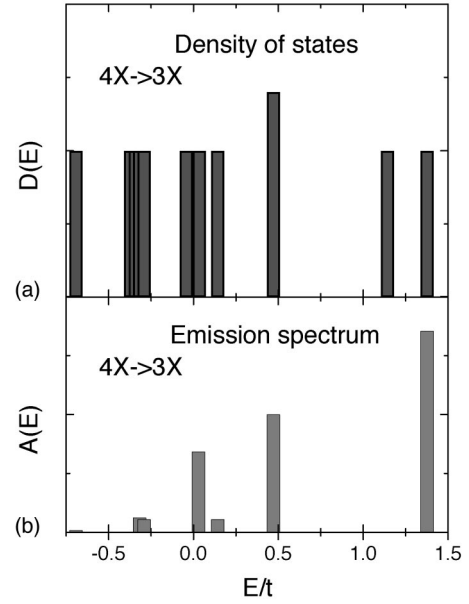


FIG. 7. (a) Density of excited states of three excitons (b) Emission spectrum from the 4X triplet-triplet ground state to the 3X ground and excited states.

$$E_{1,2} = E_s^0 + 2E_p^0 - 2V_{ee}^{sp,x},$$

$$E_{1,3} = E_s^0 + 2E_p^0 + 2V_{ee}^{pp,x} - V_{ee}^{sp,x}, \tag{14}$$

$$E_{2,2} = E_s^0 + 2E_p^0 - 2V_{ee}^{pp,x},$$

$$E_{2,3} = E_s^0 + 2E_p^0 + V_{ee}^{sp,x},$$

$$E_{3,3} = E_s^0 + 2E_p^0 + 2V_{ee}^{pp,x} + 4V_{ee}^{sp,x}.$$

The total width of the band is $6V_{ee}^{sp,x} \approx 1.5V_0$. The nine states are coupled via electron-hole scattering with the two singlet configurations $|c\rangle$ and $|d\rangle$, and with the lowest-kinetic energy configurations. The final Hamiltonian has to be diagonalized numerically. An example of the spectrum is shown in Fig. 7(a). The energy of the 3X states is measured from the energy of the triplet-triplet 4X state, i.e., decreasing energy corresponds to excited states. There are two states in a p shell plus a wide band of excited states at higher energies. The height of the bar of one state has been artificially increased. This is a single triplet-triplet 3X state, which we include here for the future comparison of the emission spectra.

To estimate the effect of mixing with the band of excited states on the ground-state energy, we give the change of the 3X ground state energy, from $2.3125t$ to $2.2201t$, for $V_0 = 0.5$. We see that the effects on the ground-state energy are small.

D. Four-exciton states

Let us start with the singlet-singlet configuration. The ground state is a linear combination of three singlet-

configurations $|a\rangle$, $|b\rangle$, and $|c\rangle$, shown in Fig. 6. Each of the three four-electron (hole) singlet states consists of a singlet in the s shell and a singlet in the p shell. To construct excited states we must promote an electron and a hole from the s

shell to the p shell. We can do this in two ways, as shown in Fig. 6. The resulting configuration must also be a pair of singlets, as indicated by arrows, to maintain total spin. The two properly symmetrized excited states are

$$\begin{aligned}
 |d\rangle &= \frac{1}{\sqrt{2}}(c_{10\uparrow}^+ c_{00\downarrow}^+ + c_{00\uparrow}^+ c_{10\downarrow}^+) \frac{1}{\sqrt{2}}(h_{10\downarrow}^+ h_{00\uparrow}^+ + h_{00\downarrow}^+ h_{10\uparrow}^+) (c_{01\uparrow}^+ c_{01\downarrow}^+) (h_{01\downarrow}^+ h_{01\uparrow}^+) |v\rangle, \\
 |e\rangle &= \frac{1}{\sqrt{2}}(c_{01\uparrow}^+ c_{00\downarrow}^+ + c_{00\uparrow}^+ c_{01\downarrow}^+) \frac{1}{\sqrt{2}}(h_{01\downarrow}^+ h_{00\uparrow}^+ + h_{00\downarrow}^+ h_{01\uparrow}^+) (c_{10\uparrow}^+ c_{10\downarrow}^+) (h_{10\downarrow}^+ h_{10\uparrow}^+) |v\rangle.
 \end{aligned} \tag{15}$$

The energy of these states equals $E_{d(e)} = E_s^0 + 3E_p^0 - (V_{ee}^{pp,x} + V_{hh}^{pp,x})$. There is only one exchange term between the two p -shell electrons and holes. The intershell exchange term between the two spin parallel electrons was canceled by the repulsive exchange energy in the s - p singlet. The ground-state energy in the absence of s - p shell mixing is $E_0 = 2E_s^0 + 2[E_p^0 - (V_{ee}^{sp,x} + V_{hh}^{sp,x})] - 2V_{eh}^{pp}$.

The two degenerate excited states are coupled by the electron-hole interaction. We form a symmetric and antisymmetric combination $|\pm\rangle = (1/\sqrt{2})(|d\rangle \pm |e\rangle)$. This leads to two eigenvalues $E_{\pm} = E_s^0 + 3E_p^0 - (V_{ee}^{pp,x} + V_{hh}^{pp,x}) \pm V_{eh}^{pp}$. Only the symmetric state couples to the ground state and renormalizes its energy:

$$\begin{pmatrix} 2E_s + 2[E_p^0 - (V_{ee}^{sp,x} + V_{hh}^{sp,x})] - 2V_{eh}^{pp} & -\sqrt{6}V_{eh}^{sp} \\ -\sqrt{6}V_{eh}^{sp} & E_s + 3E_p^0 - (V_{ee}^{pp,x} + V_{hh}^{pp,x}) - V_{eh}^{pp} \end{pmatrix}.$$

The renormalized electron-hole interaction matrix element reflects the more involved character of scattering states. It is a product of the normalization factor of the ground state, $\sqrt{3}$, and the normalization factor of the excited state, $\sqrt{2}$. The numerical form of the Hamiltonian describing the coupling of the ground and a single relevant excited state is

$$\begin{pmatrix} 6t - 4.75V_0 & -(\sqrt{6}/4)V_0 \\ -(\sqrt{6}/4)V_0 & 7t - 3.625V_0 \end{pmatrix}.$$

Let us now turn to the triplet-triplet configuration. The ground state is a singlet in the s shell and a triplet in the p shell. We must now promote an electron (hole) from the s shell to the p shell. We can do this in two ways, as shown in Fig. 6. The resulting configuration must also consist of a singlet and a triplet, the singlet now consisting of two electrons in one of the states of the p shell.

The two properly symmetrized excited states are

$$\begin{aligned}
 |a\rangle &= (c_{10\downarrow}^+ c_{00\downarrow}^+) (c_{01\uparrow}^+ c_{01\downarrow}^+) (h_{10\uparrow}^+ h_{00\uparrow}^+) (h_{01\downarrow}^+ h_{01\uparrow}^+) |v\rangle, \\
 |b\rangle &= (c_{01\downarrow}^+ c_{00\downarrow}^+) (c_{10\uparrow}^+ c_{10\downarrow}^+) (h_{01\uparrow}^+ h_{00\uparrow}^+) (h_{10\downarrow}^+ h_{10\uparrow}^+) |v\rangle.
 \end{aligned} \tag{16}$$

The energy of these states equals $E_{a(b)} = E_s^0 + 3E_p^0 - 2(V_{ee}^{sp,x} + V_{hh}^{sp,x}) - (V_{ee}^{pp,x} + V_{hh}^{pp,x})$. This energy is lowered from the corresponding excited states in the singlet-singlet configuration by the exchange energy of two s - p electrons. The ground-state energy in the absence of s - p shell mixing is $E_0 = 2E_s + 2[E_p^0 - (V_{ee}^{sp,x} + V_{hh}^{sp,x})] - 2V_{eh}^{pp}$.

The two degenerate excited states are coupled by the electron-hole interaction. We form a symmetric and antisymmetric combination $|\pm\rangle = (1/\sqrt{2})(|a\rangle \pm |b\rangle)$. This leads to two eigenvalues $E_{\pm} = E_s + 3E_p^0 - 2(V_{ee}^{sp,x} + V_{hh}^{sp,x}) - (V_{ee}^{pp,x} + V_{hh}^{pp,x}) \pm V_{eh}^{pp}$. Only the symmetric state couples to the ground state and renormalizes its energy:

$$\begin{pmatrix} 2E_s + 2(E_p^0 - (V_{ee}^{sp,x} + V_{hh}^{sp,x})) - 2V_{eh}^{pp} & -\sqrt{2}V_{eh}^{sp} \\ -\sqrt{2}V_{eh}^{sp} & E_s + 3E_p^0 - 2(V_{ee}^{sp,x} + V_{hh}^{sp,x}) - (V_{ee}^{pp,x} + V_{hh}^{pp,x}) - V_{eh}^{pp} \end{pmatrix}.$$

The final form of the Hamiltonian describing the coupling of the ground-state and a single relevant excited state is

$$\begin{pmatrix} 6t - 4.75V_0 & -(\sqrt{2}/4)V_0 \\ -(\sqrt{2}/4)V_0 & 7t - 4.625V_0 \end{pmatrix}.$$

We see that the energy of triplet excited states is lower than the energy of singlet excited states but the strength of coupling of singlet states is higher. The small energy separation of triplet excited states from the ground state leads to stronger level repulsion. This is, however, compensated for by the stronger interaction of levels in the singlet-singlet configuration, and the singlet-singlet configuration becomes the ground state. The splitting is very small. Larger splitting results from the coupling to higher shells if they are available.¹² The singlet-singlet ground-state configuration has to be contrasted with the configuration derived from Hund's rule,²⁶ which would predict the triplet-triplet configuration to be the ground state. It shows that different rules operate in excitonic atoms than in electronic ones.

VII. EXCITED STATES AND EMISSION SPECTRA

We have shown that for symmetric interactions and very large confinement the energy to remove an exciton from a partially filled p shell does not depend on the filling of the shell. Hence the emission spectrum of the p shell does not depend on the population of this shell. In order to distinguish spectra corresponding to different numbers of excitons we need to investigate removal of excitons from a filled s shell as a function of the filling of the p shell. These processes leave the final-state exciton droplet in an excited state, and hidden symmetry no longer applies. The excited states were already investigated in Sec. VI.

To calculate the emission spectrum we assume that the quantum dot is in a quasiequilibrium with a reservoir of electron-hole pairs in, e.g., the energetically higher wetting layer or 3D continuum. This determines the probability $P(N, i)$ that the dot is occupied with N electrons and is in an initial state $|N, i\rangle$. The emission spectrum is given by $E(\omega) = \sum_{N, i} P(N, i) E(\omega, N, i)$.

The emission spectrum of a dot with N electrons in a state $|i\rangle$, $E(\omega, N, i)$, is given by Fermi's golden rule in terms of exact energies and eigenstates of the initial N and final $N - 1$ exciton states:

$$E(\omega, N, i) = \sum_f |\langle f, (N-1) | P^- | N, i \rangle|^2 \delta(E_i - E_f - \omega). \quad (17)$$

If we assume fast energy relaxation, only emission spectra from ground states of N exciton complexes are needed. The calculated emission spectra are shown in Fig. 8 for a typical ratio of the Coulomb to kinetic energy $V_0/t = 0.5$.^{12,13} The 1X and 2X recombination spectrum corresponds to a single recombination line. The 2X emission is at slightly lower energy, and its amplitude is twice the exciton because there are two final exciton states, with two different spin orientations.

Let us now discuss emission spectra from the ground state of the three exciton complex. The final 2X states can be

either triplet or singlet states. The 3X ground state is well approximated by the symmetrical combination $|+\rangle = (1/\sqrt{2})(|a\rangle + |b\rangle)$. The 2X final states were given in Eq. (11), and only the biexciton state $|0\rangle$ and the symmetrical excited state are coupled. For a singlet-singlet final state we find the matrix element for the transition from the 3X ground state to the singlet final states to be given by $|\langle (2X), f | P^- | 3X \rangle|^2 = |\sqrt{2}A_0^f + A_+^f/2|^2$. We see that the contribution from the ground state is increased by a factor $\sqrt{2}$, and the coefficient of the excited state is decreased by a factor of 2 as a result of overlaps of different states. For the 2X ground state $A_0 \gg A_+$, and both coefficients are positive. This multiplicative factor enhances the contribution from the 2X ground state, i.e., recombination from the p shell. On the other hand, the excited state, corresponding to vacancies in the s shell, has $A_0 \ll A_+$ and the two coefficients have opposite sign. The smaller coefficient A_0 is enhanced by the factor $\sqrt{2}$, while the larger excited-state coefficient A_+ , with opposite sign, is reduced by a factor of 2. They become now comparable factors, and tend to cancel each other. Hence the s -shell contribution to the emission spectrum from the singlet-singlet 2X configuration is very small. What remains is the emission process where the final state is the symmetric combination of the two triplet biexciton states. Hence the 3X to 2X emission spectrum has two groups of peaks, the emission from the p shell and the emission from the s shell. The s shell emission is to the final triplet biexciton state, with energy very close to the 1X and 2X emission line. This is because we removed an exciton with such a spin configuration which did not allow for the exchange with an electron and a hole in the p shell.

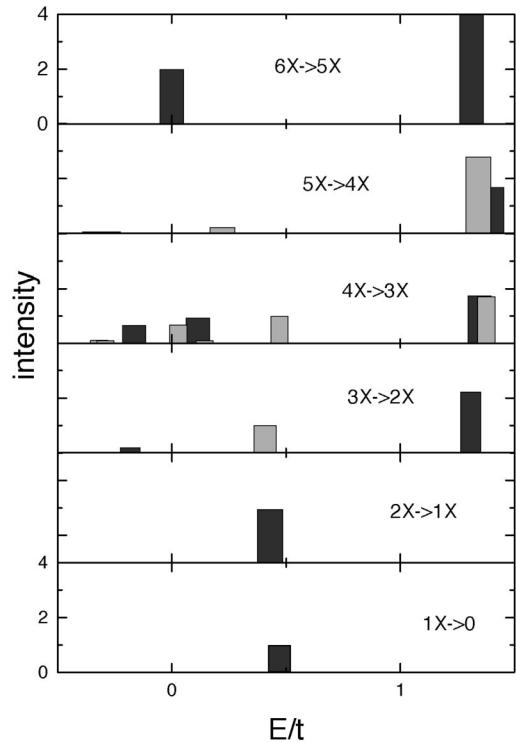


FIG. 8. Emission spectra from N exciton ground states to $(N - 1)$ exciton ground and excited states for $V_0/t = 0.5$.

The emission from the $4X$ complex to excited states of the $3X$ complex consists of two spectra originating from almost degenerate singlet-singlet and triplet-triplet initial $4X$ states. The triplet-triplet recombination spectrum, and its comparison with the final density of states, is shown in Fig. 7. The recombination spectra consists of three groups of states: (a) the recombination from the p shell which is degenerate with the recombination from the $3X$ complex, (b) the recombination to the final $3X$ triplet-triplet state, which is close in energy to the recombination from a single exciton, and (c) the lower-energy band of the $3X$ excited states, shown in detail in Fig. 7

The emission from the $5X$ complex to the singlet-singlet and triplet-triplet $4X$ final states shows a very strong emission from the p shell and a very weak emission from the s shell. The weak emission from the s shell is caused by a similar interference effect to that for the $3X$ complex. The matrix element for the recombination from the $5X$ ground state to the ground state and one excited singlet-singlet $4X$ states is given by $|\langle(4X,ss),f|P^-|5X\rangle|^2 = |\sqrt{3/2}A_0^f + A_+^f/2|^2$, where coefficients A^f are eigenvectors of the four exciton singlet-singlet Hamiltonian. Hence the recombination to the ground state is enhanced, and that to the excited state, with a missing exciton in the s shell, is reduced.

There are three triplet-triplet finite $4X$ states. Only two of them can be reached from a given initial $5X$ configuration. They have the same energy and are coupled to only one excited state but their matrix elements are different. For $S=1$ and $S_z=1$, the transition probability is $|\langle(4X,tt),f|P^-|5X\rangle|^2 = |\sqrt{2}A_0^f + A_+^f/2|^2$, where coefficients A^f are eigenvectors of the triplet-triplet four-exciton Hamiltonian.

For $S=1, S_z=0$ the transition probability is $|\langle(4X,tt),f|P^-|5X\rangle|^2 = |A_0^f/\sqrt{2} + A_+^f/2|^2$. The $S_z=0,1$ probabilities have to be added.

The final result, Fig. 8, shows that in the $5X$ complex the emission from the s shell is suppressed in comparison with the lower density quantum dot, i.e., with either four or three excitons, a rather counterintuitive result. The emission from the s shell is recovered when our dot is completely filled with $6X$. The emission from the s shell corresponds now to the removal of the s -shell exciton, without mixing with other configurations. The energy of this quasiexciton is renormalized by an exchange interaction of the s -shell electron and a hole with electrons and holes in a p shell. This lowers the energy of the emission band by the exchange self-energy of the exciton $2(V_{ee}^{sp,x} + V_{hh}^{sp,x})$.

Therefore, we see that the emission spectra as a function of the number of excitons have several characteristic features. For one and two excitons the emission takes place from the exciton and biexciton state, with electrons and holes primarily in the s shell. The energy shift between the exciton and biexciton is very small on the scale of the largest energy in the problem, i.e., the kinetic energy t . When the number of

excitons increases, extra electrons and holes populate excited states of the p shell. The recombination energy from the p -shell does not depend on the number of excitons, a result of hidden symmetry, i.e., cancellation of many processes. However, the recombination from the s shell depends on the population of the p shell. This is a rather complicated process, involving a number of excited states and peculiar interference effects in matrix elements. This interference is responsible for promoting the recombination process from three- and four-exciton complexes to spin-polarized final states. This process involves a removal of an exciton with electron and hole spins opposite to spins of electrons and holes in a partially filled p shell. Hence the energy of this recombination line is not affected by the population of the p shell, and follows the energy of an exciton. Only when the p shell begins to fill up with more than two particles, does the s -shell recombination line shift down in energy. The shift is due to exchange energy of the removed s -shell exciton with p -shell excitons. The emission to final polarized states may perhaps explain why high excitation photoluminescence emission from higher electronic shells is not accompanied by a band-gap renormalization of emission from lower shells.

VIII. SUMMARY

We have shown that the emission spectrum from a very simple and general model of a quantum dot is a sensitive function of the number of excitons in the dot. Hence “engineering” optical properties of quantum dots requires not only engineering of the single-particle levels but of many-particle states and interactions as well.

The detailed calculations of the emission spectra for up to six excitons reveal an interesting interplay of spin and correlations in the exciton droplet. The spin-polarized components of the exciton droplet lower their energy due to attractive exchange interaction. In the spin-unpolarized configurations exchange is repulsive, but the number of possible configurations increases. The mixing of configurations (correlations) due to the electron-hole scattering more than compensates for the loss of exchange. Because of correlations there appears a modulation of matrix elements in the recombination process which leads to, e.g., suppression of the recombination at low energy in the five-exciton complex and enhanced emission into spin-polarized states for low exciton numbers. This may perhaps explain the lack of significant band-gap renormalization observed in high excitation photoluminescence experiments. It is hoped that these calculations will serve as a fingerprint of excitonic artificial atoms observed in “single-dot spectroscopy.”

ACKNOWLEDGMENTS

The author acknowledges informative discussions with M. Bayer, A. Forchel, A. Wojs, S. Fafard, and G. Aers, and support from the Alexander von Humboldt Foundation.

- ¹For reviews and references, see L. Jacak, P. Hawrylak, and A. Wojs, *Quantum Dots* (Springer-Verlag, Berlin, 1998); R. C. Ashoori, *Nature* (London) **379**, 413 (1996); M. Kastner, *Phys. Today* **46**, 24 (1993); T. Chakraborty, *Comments Condens. Matter Phys.* **16**, 35 (1992).
- ²R. C. Ashoori, H. L. Stormer, J. S. Weiner, L. N. Pfeiffer, K. W. Baldwin, and K. W. West, *Phys. Rev. Lett.* **71**, 613 (1993).
- ³S. Tarucha, D. G. Austing, T. Honda, R. J. van der Hage, and L. P. Kouvehoven, *Phys. Rev. Lett.* **77**, 3613 (1996).
- ⁴P. Hawrylak, C. Gould, A. Sachrajda, Y. Feng, and Z. Wasilewski, *Phys. Rev. B* **59**, 2801 (1999).
- ⁵S. Fafard, K. Hinzer, S. Raymond, M. M. Dion, J. P. McCaffrey, Y. Feng, and S. Charbonneau, *Science* **274**, 1350 (1996).
- ⁶N. Kirstaedter, N. N. Ledentsov, M. Grundmann, D. Bimberg, V. M. Ustinov, S. S. Ruvimov, M. V. Maximov, P. S. Kop'ev, Zh. I. Alferov, U. Richter, P. Werner, U. Gösele, and J. Heydenreich, *Electron. Lett.* **30**, 1416 (1994); M. Grundmann, J. Christen, N. N. Ledentsov, J. Bohrer, D. Bimberg, S. S. Ruvimov, P. Werner, U. Richter, U. Gosele, J. Heydenreich, V. M. Ustinov, A. Yu. Egorov, A. E. Zhukov, P. S. Kop'ev, and Zh. I. Alferov, *Phys. Rev. Lett.* **74**, 4043 (1995).
- ⁷M. Bayer, T. Gutbrod, A. Forchel, V. D. Kulakovskii, A. Gorbunov, M. Michel, R. Steffen, and K. H. Wang, *Phys. Rev. B* **58**, 4740 (1998).
- ⁸Z. R. Wasilewski, S. Fafard, and J. P. McCaffrey, *10th International Conference on Molecular Beam Epitaxy, Sept. 1998, Cannes, France* [*J. Cryst. Growth.* **201/202**, 1131 (1999)].
- ⁹S. Fafard, Z. R. Wasilewski, C. Ni. Allen, D. Picard, M. Spanner, J. P. McCaffrey, and P. G. Piva, *Phys. Rev. B* **59**, 15 368 (1999); R. Leon, S. Fafard, P. G. Piva, S. Ruvimov, and Z. Liliental-Weber, *ibid.* **58**, R4262 (1998).
- ¹⁰J. M. Garcia, G. Medeiros-Ribeiro, K. Schmidt, T. Ngo, J. L. Feng, A. Lorke, J. Kotthaus, and P. M. Petroff, *Appl. Phys. Lett.* **71**, 2014 (1997).
- ¹¹A. Barenco and M. A. Dupertuis, *Phys. Rev. B* **52**, 2766 (1995).
- ¹²A. Wojs and P. Hawrylak, *Solid State Commun.* **100**, 487 (1996); P. Hawrylak and A. Wojs, *Semicond. Sci. Technol.* **11**, 1516 (1996).
- ¹³S. Raymond, P. Hawrylak, C. Gould, S. Fafard, A. Sachrajda, M. Potemski, A. Wojs, S. Charbonneau, D. Leonard, P. M. Petroff, and J. L. Merz, *Solid State Commun.* **101**, 883 (1997).
- ¹⁴A. Zrenner, M. Markmann, A. Paassen, A. L. Efros, M. Bichler, W. Wegscheider, G. Böhm, and G. Abstreiter, *Physica B* **256**, 300 (1998).
- ¹⁵E. Dekel, D. Gershoni, E. Ehrenfreund, D. Spektor, J. M. Garcia, and P. M. Petroff, *Phys. Rev. Lett.* **80**, 4991 (1998).
- ¹⁶L. Landin, M. S. Miller, M-E. Pistol, C. E. Pryor, and L. Samuelson, *Science* **280**, 262 (1998).
- ¹⁷M. Grundmann, O. Stier, and D. Bimberg, *Phys. Rev. B* **52**, 11 969 (1995).
- ¹⁸C. Pryor, *Phys. Rev. Lett.* **80**, 3579 (1998).
- ¹⁹K. H. Schmidt, G. Medeiros-Ribeiro, M. Oestreich, P. M. Petroff, and G. H. Döhler, *Phys. Rev. B* **54**, 11 346 (1996).
- ²⁰H. Drexler, D. Leonard, W. Hansen, J. P. Kotthaus, and P. M. Petroff, *Phys. Rev. Lett.* **73**, 2252 (1994); M. Fricke, A. Lorke, J. P. Kotthaus, G. Medeiros-Ribeiro, and P. M. Petroff, *Europhys. Lett.* **36**, 197 (1996).
- ²¹A. Wojs, P. Hawrylak, S. Fafard, and L. Jacak, *Phys. Rev. B* **54**, 5604 (1996).
- ²²P. Hawrylak, *Phys. Rev. Lett.* **71**, 3347 (1993).
- ²³L. Rego, P. Hawrylak, J. A. Brum, and A. Wojs, *Phys. Rev. B* **55**, 15 694 (1997).
- ²⁴A. Wojs and P. Hawrylak, *Phys. Rev. B* **51**, 10 880 (1995).
- ²⁵P. Hawrylak, *Solid State Commun.* **88**, 475 (1993).
- ²⁶A. Wojs and P. Hawrylak, *Phys. Rev. B* **55**, 13 066 (1997).